Surface Orbital Magnetic Moment of Ferromagnetic Nickel Studied by Magnetic Circular Dichroism in Ni 3p Core Level Photoemission

G. van der Laan,[1] M. A. Hoyland,[1] M. Surman,[1] C. F. J. Flipse,[2] and B. T. Thole[3]
[1]*Daresbury Laboratory, Warrington WA4 4AD, United Kingdom*
[2]*Solid State Physics, Technical University, 5600 MB Eindhoven, The Netherlands*
[3]*Materials Science Center, University of Groningen, 9747 AG Groningen, The Netherlands*
(Received 4 May 1992)

The Ni 3p photoemission of ferromagnetic nickel shows a magnetic circular dichroism which is much larger than expected from the value of the bulk orbital moment. We argue that this can only be explained when the orbital moment at the surface is strongly enhanced as predicted recently by band structure calculations.

PACS numbers: 75.30.Pd, 75.25.+z, 78.20.Ls, 79.60.Cn

The study of magnetic thin films, surfaces, and multilayers has attracted much interest since it has been predicted that the magnetic moment at the surface of a transition metal is strongly enhanced over that in the bulk [1]. The magnetic anisotropy is determined for a large part by the orbital magnetic moment and, consequently, the separation of the magnetic moment into a spin and an orbital part has become a major experimental challenge. Interesting results have been obtained using neutron diffraction, resonant magnetic scattering [2], and circular magnetic x-ray dichroism (CMXD) [3,4]. However, these techniques are not or are only weakly surface sensitive. In this Letter we show that the orbital magnetic moment can also be assessed using circular dichroism in photoemission, which is a very surface sensitive technique. In the Ni 3p photoemission of ferromagnetic nickel metal we observe a large circular dichroism. By analyzing the experimental results with an Anderson impurity model, using parameters obtained from the calculation of a large number of different core level spectra, this can be related to an increased value of the orbital magnetic moment at the surface. We explain how the enhanced moment can be understood from the behavior of the wave function at the surface. The new findings are of considerable importance for the understanding of surface magnetism.

Circular dichroism in x-ray photoelectron spectroscopy (CDXPS), which was first reported by Baumgarten *et al.* [5] in the Fe 2p core level of ferromagnetic iron, measures the difference in cross section between left and right circularly polarized x rays for the excitation of a core electron into a continuum state that has no interaction with the remaining system. It gives the correlation between the spin S_v of the valence band and the orbital momentum L_c of the core hole. The connection between the magnetic field acting on S_v and the photon polarization acting on L_c requires both spin-orbit and electrostatic interactions [6]. For deep core levels the dichroism can be calculated within a one-electron model [7]. The core-valence exchange interaction couples S_v with the core hole spin S_c and the core hole spin-orbit interaction couples S_c with L_c. In the Fe 2p [5] the spin-orbit interaction aligns S_c and L_c parallel in the $2p_{3/2}$ and antiparallel in the $2p_{1/2}$ core level. Except for the sign change between these two edges, the CDXPS spectrum will be similar to the spin-polarized 2p photoemission, which shows the correlation between S_v and S_c. The situation is more complicated for shallow core levels, where the core spin-orbit interaction is small compared to the core-valence Coulomb and exchange interactions. Here we can get a much larger dichroism by coupling L_v to S_v by 3d spin-orbit interaction, inducing a 3d orbital moment and then coupling L_v to L_c by core-valence Coulomb and exchange interactions, which makes it a many-electron effect [8].

Photoemission measurements on ferromagnetic nickel were done on beam line 1.1 of the Synchrotron Radiation Source at Daresbury. Circularly polarized x rays were obtained by inserting a horizontal slit into the beam line at inclined angular view of the tangent point of the stored electron beam. The sample was a Ni(110) single crystal, cut in the shape of a picture frame, and magnetized along the [111] directions using a coil. The nickel single crystal was cleaned by repeated cycles of Ar^+ sputtering and annealing. XPS was used to monitor the presence of contaminants. Oxygen buildup was detected only after some hours. No sulfur was found, and carbon, initially present, was removed by controlled dosing in 10^{-6} torr oxygen and flashing at 600°C. Measurements were done at room temperature with the sample in magnetic remanence and in a vacuum of $\sim 10^{-10}$ torr for not more than half an hour after cleaning. Longer measurement times resulted in a gradual decrease of the circular dichroism due to contamination of the surface.

The plane of measurement contained the [110] surface normal and the [1$\bar{1}$1] magnetization direction in the surface plane. The incident angle of the x rays was $-45°$. The photoelectrons were collected at an emission angle of 45° using a hemispherical analyzer equipped with multichannel detection. The photoemission intensities were measured with the projected photon helicity parallel (I^+) and antiparallel (I^-) to the magnetization direction.

The dichroism was calibrated by measuring the CMXD of the Ni $2p$ edge and comparing it to the measurements by Chen *et al.* [9]. This showed that the actual dichroism $I_R - I_L$ was equal to $2(I^+ - I^-)$, where the factor of 2 accounts for the angle of incidence, the incomplete circular polarization of the x rays, and the incomplete magnetization of the sample.

Figure 1 shows the Ni $3p$ photoemission intensities I^+ and I^- measured at 400-eV photon energy. The spectra are the sum over a large number of separate scans. The energy of the Fermi level was measured immediately after each scan. We found that the Fermi levels of the I^+ spectra were shifted to 40 meV lower kinetic energy compared to the I^- spectra, for which we corrected the $3p$ data. The energy shift between I^+ and I^- was 0.2 eV at the onset of the $3p$ edge. Figure 1 shows the dichroism $2(I^+ - I^-)$, which is a dispersive curve with a sharp positive peak at low binding energy and a broader structure with negative intensity at higher energies.

We compared the measured core level photoemission with calculated results using an Anderson impurity model. Such a localized approach gives a good agreement for the observed multiplet and satellite structure of nickel [10]. The parameters of this model calculation were obtained by analyzing the experimental data from different high-energy spectroscopies, such as the $3d$, $3p$, $3s$, and $2p$ photoemission, the $2p3d3d$, $2p3p3d$, $2p3s3d$, and $2p3p3p$ resonant photoemission decay, and the $3p$ and $2p$ CMXD, and x-ray absorption. The optimal ground state had d weights of 18% d^8, 49% d^9, and 33% d^{10} [10,11]. The spin-orbit coupling was quenched by using hybridization interactions having the D_3 symmetry of the valence holes, which are centered around the L point of the Brillouin zone. The quenching was needed to obtain the small L_z value of $0.053\mu_B$ required to reproduce the CMXD spectra [10]. This value agrees with neutron diffraction measurements [12] and local spin-density theory [13]. The calculated satellite intensities were strongly dependent on the d count, whereas the circular dichroism was also sensitive to the orbital magnetic moment.

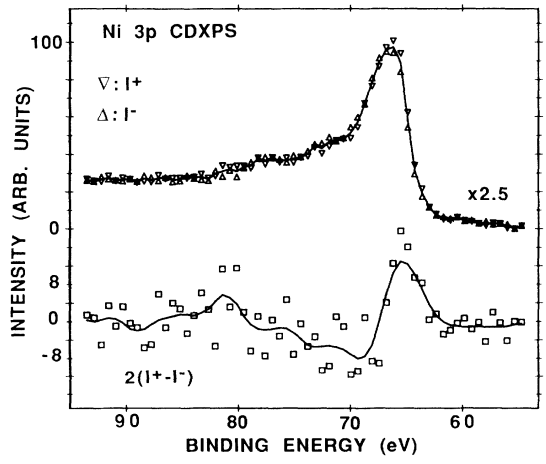

FIG. 1. Experimental Ni $3p$ photoemission intensities I^+ and I^- using circularly polarized x rays with the projected photon helicity parallel (∇) and antiparallel ($\triangle$), respectively, with the $[1\bar{1}1]$ magnetization direction in the Ni(110) surface plane. The line drawn is the isotropic spectrum. $2(I^+ - I^-)$ gives the circular magnetic dichroism $I_R - I_L$. The line drawn is a smoothed function.

The calculated Ni $3p$ XPS and CDXPS spectra are given in Figs. 2(a) and 2(b), respectively. The main peak in the XPS spectrum has primarily $3p^5d^{10}$ character. The satellite structure has mainly $3p^5d^9$ character and is split by the large $3p$-$3d$ electrostatic interaction into three peaks which are assigned as $^3F\,^1D$, $^3P\,^3D$, and $^1P\,^1F$. The measured dichroism (Fig. 1) agrees well with the predicted shape [Fig. 2(b)] but is about 4 times larger in size.

Part of this factor can be explained by the geometry of the experiment. For emission from a p core level to structureless d continuum states far above threshold, the dependence of the relative dichroism (the asymmetry) on the geometry is given by [14]

$$A(\hat{\mathbf{z}}) = \frac{4(\hat{\mathbf{q}}\cdot\hat{\mathbf{M}}) - 6(\hat{\mathbf{q}}\cdot\hat{\mathbf{z}})(\hat{\mathbf{z}}\cdot\hat{\mathbf{M}})}{5 - 3(\hat{\mathbf{q}}\cdot\hat{\mathbf{z}})}, \tag{1}$$

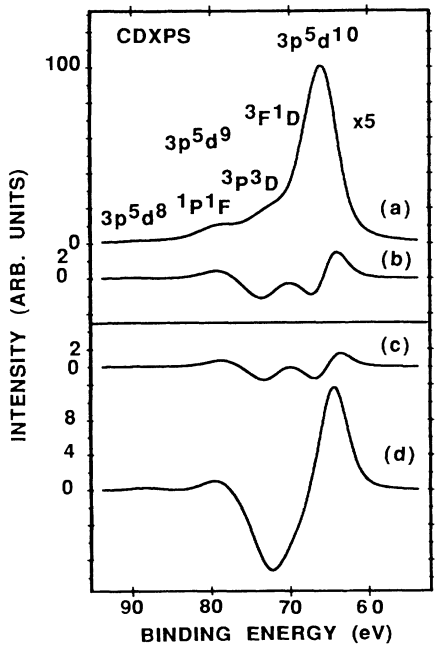

FIG. 2. Calculated results for the angular-integrated Ni $3p$ photoemission using an Anderson impurity model in D_3 symmetry for ferromagnetic nickel with d weights of 18% d^8, 49% d^9, and 33% d^{10} and an orbital magnetic moment $0.053\mu_B$. (a) XPS; (b) CDXPS; (c) CDXPS with zero $3d$ spin-orbit coupling; (d) CDXPS with spin-orbit coupling (SO_3 symmetry). The spectra were convoluted with a Lorentzian of $\Gamma = 2$ eV and a Gaussian of $\sigma = 1.33$ eV.

where $\hat{\mathbf{q}}$ is the polarization vector of the light, $\hat{\mathbf{M}}$ is the magnetization direction of the sample, and $\hat{\mathbf{z}}$ is the direction of detection of the photoelectrons. The theoretical spectra in Fig. 2 give the angle-integrated photoemission. Thus, effectively this corresponds to a value of $A(\hat{\mathbf{z}})$ where the average over all $\hat{\mathbf{z}}$ has been taken for the numerator $(I_R - I_L)$ and the denominator $(I_R + I_L)$. These averages are $2\hat{\mathbf{q}}\cdot\hat{\mathbf{M}}$ and 4, respectively, giving an effective $A(\hat{\mathbf{z}})$ of $\frac{1}{2}\hat{\mathbf{q}}\cdot\hat{\mathbf{M}} = 0.35$. Our experimental geometry corresponds to $A(\hat{\mathbf{z}}) = 0.57$ and so an increase of the dichroism by a factor of 1.6 is due to the angle dependence, leaving a factor of 2.5. Because the photoemission probes only the top few layers, we ascribe this effect to the influence of the surface. The reduction of the number of neighbors at the surface induces a narrowing of the $3d$ band, which is accompanied by an upward electrostatic shift to maintain charge neutrality [15]. This is supported by local spin-density functional calculations which predict a 13% enhancement of the Ni(110) surface magnetic moment compared to the bulk [1]. The enhancement for the orbital part of the magnetic moment will be larger than for the spin part, when the effective spin-orbit coupling increases. This is expected at the surface because the electron states are more localized. The latter is evidenced by the presence of a surface state with a large exchange interaction, as observed in spin-resolved inverse photoemission [16]. Self-consistent calculations using the muffin-tin orbitals film method show a reduced quenching of the spin-orbit coupling by the crystal field and an increase of $0.02\mu_B$ and $0.01\mu_B$ in the orbital magnetic moment for the surface and subsurface layer of nickel, respectively [17].

We will now present an analysis which shows that a strongly increased L_z value is needed to explain the magnitude of the experimental dichroism. Dichroism in core level photoemission is caused by correlation of L_c to S_v, which is produced by two mechanisms [6,8]. In the first mechanism, S_v couples to S_c by core-valence exchange interactions and then S_c couples to L_c by core spin-orbit interaction. In high-spin final states, S_v and S_c are coupled $(S_v \cdot S_c > 0)$ parallel and in low-spin states antiparallel. The core spin-orbit interaction splits the final state LS multiplets into states with an energy separation of the order of the spin-orbit coupling parameter. The high-energy states have L_c and S_c parallel and in the low-energy states they are antiparallel. Thus in the $3p$ spectrum we will see that each LS final state gives a dispersive type line with different sign for high- and low-spin states. This contribution is insensitive to the details of the ground state. It is impossible to increase this contribution substantially because the spin of the ground state, the core-valence Coulomb interactions, and the core spin-orbit interaction are already at their full strength. Excluding drastic changes in the d count, changes in the orbital part of the ground state can only give rise to shifts in intensities of at most 20%. This first contribution is shown in Fig. 2(c) which contains the spectrum in spherical symmetry without valence band spin-orbit coupling.

In the second mechanism, S_v is coupled to L_v by valence band spin-orbit coupling and L_v is coupled to L_c by core-valence Coulomb interactions. So when by spin-orbit interaction L_v has some value, then we will see this in the dichroism as a peak proportional to $\langle L_v \cdot L_c \rangle$ in the final states; i.e., states with a high L value give a peak with a sign opposite to those with a low L value. So, e.g., in our Ni calculation, L_v and L_c are parallel, weakly, and strongly antiparallel in the F, D, and P final states. In total this contribution gives a spectrum that is roughly proportional to L_v because the coupling between L_v and L_c (producing the splitting between the LS multiplets) is produced by Coulomb interactions which we have no freedom to increase. The maximum size of this contribution is shown in Fig. 2(d) which is obtained from Fig. 2(c) by including spin-orbit coupling giving a $^3F_4$ ground state with $L_z = 1.8\mu_B$ per hole. L_v is very sensitive to the orbital symmetry and degeneracy. In the bulk ground state the orbital momentum per hole is quenched from about $1.8\mu_B$ in the $^3F_4$ ground state in spherical symmetry to $0.053\mu_B$ in the mainly $^3A_1$ state of our D_3 calculation. Therefore, in the calculated bulk spectrum the contribution of the second mechanism is negligible. Because the contribution from the first mechanism is constant, the second contribution has to grow by a large factor in order to get any appreciable increase of the spectrum. A factor of 2 to 3 is the only way to explain the magnitude of the experimental spectrum. In order to get a factor like this we need a ground state consisting of $^3T_1$ or $^3T_2$ of d^8 and $^2T_2$ of d^9 in tetrahedral symmetry, which amounts to assuming that the t_2 type d functions are degenerate or only a few tenths of an eV apart. Thus the decrease of the site symmetry at the surface leads to an apparent increase of the symmetry of the wave function. We could explain this in band structure terms as follows: In the bulk the holes are forced into the low symmetry L point because this is the point of highest energy in the valence band, having the most unfavorable interactions with the neighbors. This is why we need the D_3 symmetry of the L point to obtain the low L_z value of the bulk. At the surface apparently the orbitals with L point symmetry are no longer highest in energy and those with the high Γ point symmetry now contain the holes. Whatever may be the case, we absolutely need degeneracy of the unoccupied orbitals to obtain a reasonable L_z value. It would be interesting to see whether and under what circumstances a large value for L_z can be obtained from band structure calculations.

Concluding we may say that, although a detailed analysis of the Ni $3p$ CDXPS is hampered by the poor statistics because the production of circularly polarized radiation can only be achieved at the expense of intensity, it is clear that an interesting effect is observed. The experimental shape agrees qualitatively with the predicted

bulk spectrum, but the absolute magnitude indicates a large orbital momentum. This information obtained from the CDXPS of a shallow core (or valence) level is unique and there is no other technique that can be used to check the results. CMXD, x-ray resonant magnetic scattering, and neutron diffraction give the bulk orbital magnetic moment, unless the surface to bulk ratio is very large, whereas spin-resolved (inverse) photoemission mainly gives the spin contribution.

Measurements of the magnetic circular dichroism increase the information that can be obtained from photoemission from core levels with large core-valence interactions. CDXPS can be used to study the interactions which determine the magnitude of the orbital magnetic moment, such as spin-orbit interaction, Coulomb interaction, hybridization, and crystal fields. The technique is a unique tool to study the magnetic properties of surfaces and thin layers, where the reduced coordination and the electron localization modify the orbital momentum. However, the experiments require an extremely bright x-ray source with a high degree of circular polarization. For Ni(110) we obtained a larger orbital momentum from photoemission than from x-ray absorption, which suggests a surface effect. Further study of the dichroism as a function of depth can be made by tuning the photon energy in photoemission, or by using partial yield in x-ray absorption. The large orbital contribution to the magnetic moment refutes the old hypothesis of magnetically dead layers, but is in agreement with band structure calculations that predict an enhancement in the magnetic moment. We suggested that the orbital contribution, which is $\sim 10\%$ in the bulk, increases strongly at the surface due to increased localization.

[1] H. Krakauer, A. J. Freeman, and E. Wimmer, Phys. Rev. B **28**, 610 (1983).
[2] D. Gibbs, D. R. Harshman, E. D. Isaacs, D. B. McWhan, D. Mills, and C. Vettier, Phys. Rev. Lett. **61**, 1241 (1988).
[3] B. T. Thole, P. Carra, F. Sette, and G. van der Laan, Phys. Rev. Lett. **68**, 1943 (1992).
[4] Y. Wu, J. Stöhr, B. D. Hermsmeier, M. G. Samant, and D. Weller, Phys. Rev. Lett. **69**, 2307 (1992).
[5] L. Baumgarten, C. M. Schneider, H. Petersen, F. Schäfers, and J. Kirschner, Phys. Rev. Lett. **65**, 492 (1990).
[6] G. van der Laan, Phys. Rev. Lett. **66**, 2527 (1991).
[7] H. Ebert, L. Baumgarten, C. M. Schneider, and J. Kirschner, Phys. Rev. B **44**, 4406 (1991).
[8] B. T. Thole and G. van der Laan, Phys. Rev. B **44**, 12424 (1991); Phys. Rev. Lett. **67**, 3306 (1991).
[9] C. T. Chen, F. Sette, Y. Ma, and S. Modesti, Phys. Rev. B **42**, 7262 (1990).
[10] G. van der Laan and B. T. Thole, J. Phys. Condens. Matter **4**, 4181 (1992).
[11] G. van der Laan, M. Surman, M. A. Hoyland, C. F. J. Flipse, B. T. Thole, H. Ogasawara, Y. Seino, and A. Kotani, Phys. Rev. B **46**, 9336 (1992).
[12] P. J. Brown, J. Phys. I (France) **1**, 1529 (1991).
[13] O. Ericksson, B. Johansson, R. C. Albers, A. M. Boring, and M. S. S. Brooks, Phys. Rev. B **41**, 11807 (1990); **42**, 2707 (1990).
[14] C. M. Schneider, D. Venus, and J. Kirschner, Phys. Rev. B **45**, 5041 (1992).
[15] M. Weinert and J. W. Davenport, Phys. Rev. Lett. **54**, 1547 (1985).
[16] M. Donath, V. Dose, K. Ertl, and U. Kolac, Phys. Rev. B **41**, 5509 (1990).
[17] O. Ericksson, G. W. Fernando, R. C. Albers, and A. M. Boring, Solid State Commun. **78**, 801 (1991).